Particulate metal composites as backing for ultrasonictransducers for continuous non-destructivemeasurements at moderate and high temperatures

Redha Boubenia, Eric Rosenkrantz, Florence Despetis, Philippe Combette, Jean-Yves Ferrandis

> MANUSCRIPT NO. TUFFC-10055-2020.R1<

Particulate metal composites as backing for ultrasonic transducers for continuous non-destructive measurements at moderate and high temperatures

R. Boubenia, E. Rosenkrantz, F. Despetis, P. Combette and, J-Y. Ferrandis.

***Abstract* – There is an increasing need for ultrasonic transducers able to operate continuously at high temperatures in many industrial sectors. Operating temperatures may be 600 °C and higher. There isn't any commercial solution to deal with such applications and only few ultrasonic prototype probes exist. It is therefore important to find new materials suitable for the manufacture of high-temperature ultrasonic probes. One important element of ultrasonic probes is the backing as it enables the control of both sensitivity and bandwidth. The goal of this paper is to explore the possibility of using particulate metal composite as a high-temperature backing elements. Several tin-tungsten composites with different tungsten volume fractions were produced by uniaxial pressing. The backings were characterized by ultrasonic spectroscopy. The backings have an impedance ranging from 25 to 31 MRayl with attenuation at least equal to 20 dB/cm and up to 191 dB/cm. In order to operate at 600 °C, a sample of Al/W composite was produced. Its impedance ranged from 8 to 10 MRayl with a mean attenuation of around 156 dB/cm at 4.5 MHz. The metallic composites therefore have ultrasonic properties suitable for use as backing. Moreover, they are relatively easy to manufacture. These are therefore very interesting materials for high-temperature ultrasonic probe applications.**

Index Terms— Ultrasonic transducers, backing, metal composites, high-temperature, tin-tungsten, aluminum-tungsten

I. INTRODUCTION

A. Context

Many industrial processes are carried out at high temperatures and even under such conditions non-destructive testing is imperative. However, it is of course much more difficult to operate under these conditions.

As there are already commercial ultrasonic transducers for applications <300 °C, we arbitrarily qualify as moderate temperatures, the temperature range between 50° and 300 °C and as high temperatures everything above the aforementioned range. It should be noted that for most ultrasonic probe manufacturers a temperature above 50 °C is considered to be a high temperature.

Ultrasonic, non-destructive testing is one of the most widely used and the need for and development of high-performance ultrasonic probes that can operate at high temperatures is increasing. For example, in the nuclear field for the control of steam pipes [1], or for the inspection of safety devices which for future 4th generation reactors must be carried out through hot liquid, metal pipes (with θ <300 °C when the reactor is shut down and θ up to around 600 °C when the reactor is in operation [2]). Ultrasonic inspection at high temperatures is also necessary in the oil industry for example for inspections of borehole cementation where conditions of measurement are harsh with pressures around 1,400 bar and temperatures close to 200 °C [3], as well as in the chemical or pharmaceutical industry for inspection in discharge pipes or even, more generally, for the overall monitoring of high-temperature industrial processes (e.g. extrusion, forging process) [4]. There are so many applications that it therefore makes sense to find commercial solutions that partially address these issues.

B. High temperature commercial ultrasonic transducers

Above 200 °C, Electromagnetic Acoustic Transducers (EMAT) are the ultrasonic transducer most commonly used. By operating without contact, the use of EMAT does not suffer from the coupling problems inherent to the use of piezoelectric transducers and allows control at temperatures up to 600 °C. However, only electrically conductive materials can be tested and, in comparison with piezoelectric transducers, they have very a low efficiency [5]. Furthermore, most EMAT operate with permanent magnets with low Curie points (e.g. 100–150°C) requiring active cooling, or using air-cored electromagnet [6]

Most commercial solutions consist in not subjecting the active elements of the probes to high temperatures by moving measurement away using delay lines (generally made of clad rods) and, if necessary, by cooling these delay lines or else the assembly itself. Moreover, buffer rods induce systematically non-desirable acoustic dispersion effects and cause spacing problems. Furthermore, and despite this, measurements must always be carried out in a relatively short time [7].

By selecting the proper materials, even with some epoxy resins, and choosing suitable solders, the commercial piezoelectric transducers are able to work up to about 200 °C continuously. By adding delay lines, one can extend the operating temperature and time of use, but even at these moderate temperatures, because these probes contain polymer and materials such as epoxy materials, their reliability and durability are not very good. They suffer permanent damage due to internal separation caused by the difference in thermal expansion between each element of the probes, in particular between the ceramic and polymer components. Furthermore, even at moderate temperatures (about 200 °C), due to the fact that all commercial transducers contain organic matter, none are suitable for control purposes in a harsh nuclear environment e.g. near a reactor in operation where neutronic fluxes are high. However, this type of probe is of great interest in experimental nuclear reactors [8, 9] to conduct research in the general context of improving nuclear safety, optimizing fuel use…

Poor performance of commercial sensors at moderate temperatures is still a significant obstacle in many applications and no commercial ultrasonic transducers exits that can operate continuously at the target temperatures range of 500–600°C.

C. High-temperature prototype ultrasonic transducers

The difficulties when dealing with the manufacturing of high-temperature, ultrasonic transducers lie not only in finding materials (especially of the piezoelectric type) that can operate at high temperatures, but also in finding compatibility between materials and assembly techniques [1, 4]. At these temperatures, the possible differences between the thermal expansion coefficients induce significant stresses between the various components of the probe which inevitably leads to separation in the long term. This is why it is very important to choose materials that are compatible with each other and to find mechanical coupling solutions that can resist these temperatures, especially temperature variations (during return to room temperature, for example). Thus, the main problems are, on the one hand, guaranteeing mechanical resistance of the various components of the probe with each other and also ensuring the acoustic coupling of the probe with the material to be tested (e.g. by using high-temperature, ultrasonic coupling gel, dry coupling or brazed coupling for permanent structural health monitoring applications). There are solutions that partly address these issues, and therefore, prototypes of ultrasound probes do exits which can operate continuously at high temperatures [5, 10].

The main obstacle to the manufacture of high-temperature ultrasound probes is therefore not finding piezoelectric material able to operate at high temperatures as many such materials exit. There are many applications where one finds piezoelectric materials suitable for manufacture of high-temperature ultrasonic transducers. As examples, some accelerometers based on monocrystalline yttrium calcium oxyborate (YCOB) [11] and surface acoustic wave probes (SAW) using gallium orthophosphate ($GaPO_4$) crystal [12], both showed adequate thermal resistance up to 900 °C and 800 °C respectively. Piezoelectric films of AIN were successfully used up to 1000 °C to monitor the manufacturing processes for high-temperature ceramics [13]. One can note that AIN is not a ferroelectric material and its limitation is due to its fusion temperature. There are therefore many ferroelectric/piezoelectric materials with high Curie temperatures able to operate at moderate or high temperatures [4, 5, 14-16]. Indeed, rule of thumb dictates that the operating temperature of a ferroelectric piezoelectric material is about 2/3 of its Curie temperature due to the fact that the higher the Curie temperature, the lower the electromechanical coupling factors. Piezoelectric materials must therefore be chosen carefully according to the operating temperature.

In his review, Kažys cites the following materials: bismuth titanate $Bi_4Ti_3O_{12}$ (BIT); modified BIT; lead metaniobate; BIT/PZT film (applied by sol-gel technology) as the most suitable piezoelectric materials for operation at high temperatures [5]. Nevertheless, because it has a very high Curie temperature with an acceptable coupling factor (TC = 1150 °C, kt =0.30 [17]) lithium niobate ($LiNbO_3$) remains one of the most commonly used piezoelectric materials despite the fact that at 600 °C it begins to lose oxygen.

There are hence many ferroelectric/piezoelectric materials possessing high Curie temperatures, but their piezoelectric response is generally low in comparison to PZT ceramics which remain suitable for many applications at moderate and high temperatures e.g. PZT-5A (pz27 Ferroperm) and K15 (Pz46 Ferroperm) ceramics.

Some prototypes of ultrasound transducers exist using these piezoelectric materials. For most structural health monitoring (SHM) applications, ultrasonic sensors are glued on materials under test. In addition to the difficulties associated with high temperatures, the shape of the structures to be tested is generally not flat and consequently existing soldering or bonding solutions are unusable. To overcome these problems, some authors propose depositing of the piezoelectric elements directly on the test object either using CVD [13], spray coating [18, 19] process or by sol-gel depositing. Several types of sol-gel composites have been developed for applications in various temperature ranges: PZT/PZT for temperatures up to 200 °C, BIT/PZT for temperatures up to 500 °C, and lithium niobate/PZT for temperatures up to at least 800 °C [4]. Despite the fact that there is no backing, sol-gel solutions produce echoes with acceptable temporal resolutions. However, the performance of these probes remains low and, above all, no feedback is available concerning the durability of this type of solution [5].

Recently, piezoelectric elements made of sodium bismuth titanate (NBT, chemical formula $Na_{0.5}Bi_{4.5}Ti_4O_{15}$, with a Curie temperature of 650 °C) were deposited using the screen-printing technique on 700 µm thick alumina plates [20]. Several ultrasonic sensors produced using this process have successfully operated at up to 350 °C. As it is not only specific to depositing on flat surfaces, this new technique appears to be a good alternative to sol-gel solutions. It also seems very promising because it allows depositing of successive layers (electrodes, brazing and mechanical adaptation layers to absorb stresses…) which would solve the main problems of acoustic and mechanical coupling between the various components of the probe. It is therefore also possible to consider deposing on backings.

The previous discussions only concern acoustic solutions involving an active element and an imposed front layer (thus not optimized), the front layers being either the material to be tested (as for SHM applications) or a protection layer. In fact, there are very few high-temperature ultrasonic sensors with optimized front matching layers and backings [21-24]

Parks et *al* tested three types of piezoelectric materials: $YCa_4O(BO_3)_3$, $LiNbO_3$, and AIN. They were studied for their use in ultrasonic transducers with an objective to operate 55 hours at 550 °C. Sintered porous carbon-carbon composite materials were used as backing. However, no particular care

has been taken to optimize them or match the layer. This layer was only intended to protect the piezoelectric element and the sensor was encapsulated within a closed cylinder [21].

Amini et *al* have manufactured several ultrasonic transducers based on lithium niobate crystals which have been soldered to porous ceramics used as backing. Some tests were also carried out using GaPO4, but no brazing alloys or adhesives were able to bond the GaPO4 crystals with porous ceramics [23, 25]. This confirms that one of the main problems in the manufacture of ultrasonic transducers dedicated to high-temperature applications is creation of the mechanical coupling. The authors paid attention to manufacture and optimize the backing layers to achieve the desired simulated performance. Porous ceramics (made of yttria-stabilized zirconia – YSZ) were manufactured using polyethylene (PE) spheres as pore-forming agents; the sphere diameter and volume fraction enabled obtaining the desired attenuation and acoustic impedance. These porous backings had acceptable attenuation of around 20–60 dB/cm in the frequency range 1.5-4.5 MHz. However, this type of material is complicated to manufacture (choice of blowing agents, sintering process, etc.) and requires complex and expensive equipment, including furnaces able to achieve very high temperatures for sintering operations in a reducing atmosphere. Moreover, it is not easy to bind them to piezoelectric materials even though they possess thermal expansion coefficients relatively close to those of the piezoelectric elements.

As it allows control of both frequency bandwidth and sensitivity of the transducer, the backing is a key component in ultrasonic probes. It is therefore very important to find new backing materials suitable for high-temperature operation. To do so, we chose to investigate the possible use of particulate metal composites as backing elements.

II. METAL COMPOSITE AS BACKING ELEMENTS FOR HIGH TEMPERATURE OPERATION

A standard ultrasonic transducer is composed of three elements. To begin with, an active element, such a solid piezoelectric ceramic (PZT) or an epoxy/ceramic composite, is used to generate an ultrasonic wave. It is worth noting that for high-temperature applications, the active element is generally a solid element such a PZT ceramic or a piezoelectric single crystal. In order to inject as much sound power as possible, an impedance matching layer is placed on the front face of the probe. Finally, a backing layer is placed on the rear surface of the piezoelectric element.

The simplest matching layer is a quarter-wave thick layer (at the center frequency). For a thick airbacked piezoelectric material (such as it can be considered as being semi-infinite) the optimal matching layer impedance is equal to $\sqrt{Z_p \times Z_m}$ whereby Z_p and Z_m are respectively the acoustic impedance of the PZT and that of the material to be tested. If one takes into account the thickness of the piezoelectric material, the optimal matching layer impedance is equal to $\sqrt[3]{Z_p \times Z_m^2}$ [27]. For typical backings, the optimal matching layer impedance is between these two values. However, such a layer only allows the acoustic impedance to be adapted near the center frequency of the transducer. By using several matching layers, one can increase the injection bandwidth and thus improve the temporal resolution by reducing the emitted wave duration [26, 27].

By absorbing the acoustic energy radiated at the rear, the backing reduces the ringing within the piezoelectric element, thus increasing the transducer bandwidth [28]. It is worth noting that it is also important to tune the electrical input of transducers to control and improve the performance of ultrasonic probes. We refer the reader to the works of Silk [29] for a general discussion on the optimal design of ultrasonic probes.

If the absorption of backing elements is too low, parasitic back-wall echoes preventing satisfactory measurements occur and will need to be eliminated. To do this, the rule of thumb is that the backing must have around 40 to 100 dB absorption depending on the transducer sensitivity. Here to have a backing of acceptable size, one assumes that attenuation (over the frequency bandwidth of the transducer) of around 10 dB/cm is sufficient [22, 29 (p60)]. In this case, a 20 mm thick backing meets this condition. Of course, if the attenuation is greater than 10 dB/cm, the size of the backing may be reduced (and thus that of the probes) and can be, for some application, a major advantage, especially for SHM applications where spacing problems are often encountered.

The simplest backing is air backing (with an impedance close to zero), in this case all the energy is directed to the front of the transducer. The sensitivity of the transducer is at a maximum, but with a small bandwidth. Due to ringing within the piezoelectric material, the duration of echoes is large [30]. When backing with air is used, the thickness of the air layer is therefore not critical. The closer the impedance of the backing is to the impedance of the piezoelectric, the more acoustic energy is transmitted through it and absorbed. This has the effect of damping the back-end signal from the ceramic element and increasing the bandwidth, at the expense of sensitivity however. A compromise must be made when choosing the acoustic impedance of the backing [30, 31].

Backings are thus very attenuating materials made of particulate composites or porous materials [29, 32]. Standard composite backings contain a small amount of filler (randomly distributed) in a polymer matrix. Such composites have a 0–3 connectivity pattern. Commonly, fillers such as tungsten, iron, magnesium, aluminum and alumina are used to obtain a high acoustic impedance. Porous material and fillers such as glass, wood and cork are used for low acoustic impedance backings. The greater the difference between the acoustic impedance of the filler and the matrix, the more acoustic energy will be absorbed by multiple scattering. For instance, if the filler is a metal and the matrix is a polymer, then the fact that the impedance of the inclusion is much higher than the matrix

impedance, the metal acts as a scatterer. In porous materials since the pores have a negligible acoustic impedance compared to that of the matrix, it is the pores that act as scatterers. The impedance ratio between the matrix and the inclusions and the size and volume fraction of inclusions enable the acoustic characteristics of the backing material to be controlled and the desired characteristics obtained (attenuation and impedance).

High-sensitivity transducers, in which the major part of the energy is directed to the front surface of the transducer, require low-acoustic impedance backings composed of porous materials. For example, porous backings are produced by compressing a mixture of metal and polymer, such as tungsten with PMMA microspheres. The polymer is then removed by burning in a furnace [32]. These porous backings also serve to damp piezoelectric composites that have a much lower acoustic impedance than solid piezoelectric.

To obtain transducers with greater damping, backings with a higher acoustic impedance will be required. The most common materials used are polymer-loaded metals, such epoxy-tungsten composites. The impedance ratio is very high and provides a high attenuation value between 40 dB/cm and 240 dB/cm for impedances ranging from 5 to 10 MRayl [32]. However, to obtain highly damped transducers, the acoustic impedance of the backing must be close to the impedance of the active elements. When using epoxy-tungsten composites, a high-volume fraction of tungsten (up to 75%) is necessary which subsequently produces a sedimentation phenomenon the porosity of which is difficult to control.

To partially overcome these problems, backings were made by mixing and compressing different types of polymer powders with metal powders e.g. vinyl/tungsten [33], polyvinyl/tungsten [34], or polymetacrylate/stainless steel 303L [35]. However, there are still problems with manufacturing reproducibility, especially for high-impedance backings. To solve this problem, it has been proposed to use three-phase metallic polymeric metal composites such as PMMA/InPb/Al [35], or composites made only of metals [31, 36].

Sayers proposes to use tin, aluminum or copper composites filled with tungsten inclusions [31]. This theoretical work provides some estimates of acoustic impedance as a function of the volume fraction of tungsten, but unfortunately no estimate of attenuation. Rokhlin manufactured tin-tungsten composites by uniaxial compression at room temperature and 220 °C [36]. For fine-tuning of the acoustic impedance, some composites of three-metal powders (tin/iron/tungsten) were produced. The effects of pressure and temperature were studied. The main conclusion is that it is preferable to compress at room temperature and a pressure of 5 kbar is sufficient to obtain dense pellets up to 70% per mass of tungsten. It is necessary to increase to 10 kbar in order to obtain denser samples up to 90% per mass of tungsten. This work contains very few acoustic results and only the impedance values as a function of the compression value are given. It does not suggest that metal composites may be used as backing material for high-temperature applications. As they are limited only by their melting temperature, we chose to continue and complete these works with the aim of using these metal composites at high temperatures. The metal backings can be used as a rear electrode or can be easily soldered to a rear electrode. In addition, metallic materials have low thermal expansion coefficients and correspond in reality to those of electrodes. Most metallic materials are suitable for nuclear applications.

We have produced several tin/tungsten samples. We chose to begin with the production of these composites because the malleability of tin renders their manufacture relatively easy. The samples were manufactured with relatively limited means: a handcrafted die, a mixer and a press. We used two tungsten granulometries in order to study the influence of the inclusion size of tungsten on the acoustic properties of the samples. For each sample, we measured the density and velocity from which the impedance and attenuation are deduced. The experimental values were compared to simple models. In addition, the aim being to offer acoustic solutions for applications up to 600°C, at the end of this paper we present a preliminary test on a tungsten-aluminum sample.

III. METAL COMPOSITE MANUFACTURING TECHNIQUE

A. Backing specifications

The backing materials used for the present study are intended to operate with the following piezoelectric elements (table 1):

Commercial denomination	Navy or standard denomination	Curie temperature (°C)	Maximal operating temperature (°C)
Pz27 (Ferroperm)	PZT5A	350	230
Pz46 (Ferroperm)	K15	650	500
X	LiNbO3 (36° Y cut)	1150	600

Table1: The three piezoelectric elements targeted, with the Curie temperature and maximal operating temperature.

The backings must meet the following specifications. The targeted operating frequency range is: 3–7 MHz. All the acoustic properties were therefore measured over this range. As already indicated above, the attenuation must be at least equal to 10 dB/cm. To specify the ultrasonic impedance range of backings, depending on which of the three piezoelectric materials is used, several simulations were carried out using a KLM model.

As a typical application, we chose to carry out a test in contact of a steel element having an acoustic impedance of Z_m = 45 MRayl. The model includes a quarter-wave layer with impedance of $Z_f = \sqrt{Z_p \cdot Z_m}$ (whereby the subscript f stands for front) and the electrical port is tuned with a generator impedance equal to $R_0 = 1/(C_0 \cdot \omega_0)$. This electrical matching provides a good compromise between the increase in bandwidth and the decrease in sensitivity [37].

The output pressure was calculated for different backing impedance values Zb ranging from 0 MRayl to 35 MRayl in steps of 5 MRayl. The applied voltage is one volt, one thus obtains the transfer function (in Pa/Volt) from which one deduces the central frequency and the fractional bandwidth of the probe at -3 and -6 dB. We then defined a sensitivity parameter (representative of the decrease in maximal output pressure while the backing impedance increases) as follows. As our aim is to design a backing element operating within 3 MHz and 7 MHz, the simulations were carried out for a 5 MHz central frequency, with the thickness of the piezo-element being equal to a half wavelength at this frequency. The results of simulations are reported in table 2. This table also indicates the properties of piezoelectric materials required for simulations:

$LiNbO_3$ Z = 34.2 MRayl; ρ = 4,64 g/cm^3; v = 7360 m/s; $Q_m = 10^4$; kt = 0.48; $\varepsilon / \varepsilon_0 = 39$; Qe = 10^3								
Z_B (MRayl)	0	5	10	15	20	25	30	35
fc (MHz)	4.69	4.65	4.60	4.55	4.48	4.38	4.23	4.00
BW% @ -3dB	76	78	80	84	89	96	106	119
BW% @ -6dB	109	111	112	117	123	132	144	160
S (%)	100	87	78	70	64	59	54	51
Pz27 Z = 33.2 MRayl; ρ = 7,70 g/cm^3; v = 4324 m/s; Q_m = 74; kt = 0.469; $\varepsilon / \varepsilon_0$=1800; Q_c = 59								
Z_B (MRayl)	0	5	10	15	20	25	30	35
fc (MHz)	4,72	4,68	4,63	4,58	4,50	4,39	4,23	3,97
BW% @ -3dB	77	78	80	84	90	97	108	122
BW% @ -6dB	110	111	112	117	124	133	145	163
S%	100	87	77	70	63	58	54	51
Pz46 Zp=26,8 MRayl; ρ = 6,53 g/cm^3; v = 4104 m/s; Q_m = 4100; kt = 0.24; $\varepsilon / \varepsilon_0$ = 39; Q_c = 250								
Z_B (MRayl)	0	5	10	15	20	25	30	35
fc (MHz)	4,77	4,72	4,66	4,57	4,43	4,20	3,85	x
BW% @ -3dB	76	77	80	86	95	108	126	x
BW% @ -6dB	110	111	114	121	131	147	168	x
S (%)	100	84	73	65	58	53	50	x

Table 2: Impedance range of backings for the three chosen piezoelectric elements. BW is the relative bandwidth and S the sensitivity ratio to the maximal pressure for Zb=0 MRayl. Data is available in [38-41]

As anticipated, one can note that, while the backing impedance increases, the bandwidth increases at the expense of sensitivity and it can be seen that the central frequency shifts toward lower frequencies. It was noted that a backing impedance between 20 MRayl and 30 MRayl resulted in a transducer having a bandwidth, at -3 dB, between 89 and 108% for both the LiNbO3 and Pz27 materials. These results are in agreement with those previously obtained [22]. Nevertheless, the output pressure is about 5 times greater for Pz27 than for LiNbO3. Transducers based on Pz27 with Sn/W backings materials would be very interesting for applications below 230 °C. Above this value, one can use the piezoelectric elements LiNbO3 and Pz46. Backing elements coupled with Pz46 materials having an acoustic impedance between 15 MRayl and 25 MRayl would produce a signal with a bandwidth of 86% to 108% at -3 dB. One notes that the pressure with Pz46 is 18% lower than the pressure induced by the LiNbO3. These impedance values are in agreement with an empirical rule for high bandwidth transducers which states that backing must have an impedance between 60% and 80% of the piezoelectric material impedance [29 (p39)].

It should be noted that a backing impedance between 5 and 15 MRayl would allow manufacturing of transducers with a higher sensitivity and an acceptable bandwidth of about 80%. This type of backing can be achieved with Al/W materials.

B. Manufacturing process

To establish the manufacturing protocol, we first made seven samples with pure white tin. The characteristics of the tin powder are as follows: 99.5% purity, average grain size equal to 149 µm, theoretical density equal to 7.265 g/cm^3. These samples were also used to determine the ultrasonic attenuation of a pure tin matrix.

The samples were manufactured by uniaxial double action compression which provides a more homogeneous compression gradient within the pellet than simple action compression [42]. The desired quantity of tin powder is introduced into a die with an interior diameter of 16 mm. This diameter has been chosen to allow acoustic characterization of the samples by ensuring the entire acoustic beam passes through them.

The samples were loaded for unidirectional axial compression using a universal test apparatus enabling control of the displacement rate. The applied load was measured with a loading cell with a maximum load of 25 T with an accuracy of around 10 kg. There are three main parameters to be controlled during compression: pressure, compression speed and temperature. The compression speed must be slow enough to enable rearranging of powder grains at the beginning of the compression process. The pressure must be sufficient to attain plastic deformation within the whole pellet in order to densify the samples and obtain samples of good mechanical resistance. However, during axial compression, lateral deformation occurs and the higher the pressure, the higher the radial stress, making it difficult to eject the pellet from the die. Samples are often damaged or broken at this stage. A compromise must therefore be found. We tested several compression configurations at various speeds, pressures and temperatures (25 °C-100 °C). Finally, the manufacturing protocol used is as follows:

- Compression force 80 kN.
- Compression speed 0.1 mm/min.
- Room temperature.

Compression is stopped when the load attains 80 kN, corresponding to a pressure of around 4 kbar. According to former works [36], this pressure enables densification of pellets up to 60% per volume of tungsten. We have found no interest in maintaining the load, but we repeat the compression process three times while allowing the mechanical stresses time to relax between each compression.

Using the same protocol as for the tin samples, we produced 17 tin/tungsten samples with two different powder grain sizes for tungsten with volume fractions of tungsten ranging from 5% to 30%. The first tungsten powder had a grain size G1 ranging from 44 µm to 74 µm and the second G2 ranging from 149 µm to 250 µm. To determine the manufacturing reproducibility, we manufactured two samples for each volume fraction, except for the 30% volume fraction for which three samples were made. Indeed, the more the volume fraction increases the more difficult it becomes to manufacture samples. The samples with a volume fraction equal to 30% are good indicators of process reproducibility.

To determine the amount of powder to be weighed, we set the final thickness of samples at 4 mm. The thickness must be sufficient to enable separation of two back wall echoes. The mass of tungsten and tin being respectively: $m_W = \rho_W \cdot \delta \cdot V$ and $m_{SN} = \rho_{SN} \cdot (1-\delta) \cdot V$, whereby, ρ_W and ρ_{SN} are respectively the theoretical density of tungsten and tin. V is the volume of samples 4 mm thick and 16 mm in diameter whereas δ is the volume fraction of tungsten. The characteristics of the sample are listed in table 3.

IV. Characterization of Backing Materials

A. Density and volume fraction estimation

The density of samples was measured using the double weighing method. Based on the density, one deduces the compactness (C) and the actual tungsten volume fraction (δ).

The mean experimental density of the seven tin pellets is equal to 7.233 g.cm^{-3} and the mean compactness ratio equal to 99.56%. The relative difference with the theoretical value (equal to 7.265 g.cm^{-3}) is 0.44%, which is negligible. The compactness is defined below.

The experimental density values of tin-tungsten samples were compared with the theoretical density given by the following relation:

$$\rho = \delta \cdot \rho_W + (1-\delta) \cdot \rho_{SN} \quad (1)$$

δ is the theoretical (desired) volume fraction of tungsten, ρ_W is the theoretical value of tungsten density equal to 19.3 g.cm^{-3} and ρ_{SN} is the theoretical value of white tin density equal to 7.265 g.cm^{-3}. The results are shown in figure 1. One notes a very good correlation between the theoretical values and the experimental values with a relative error of less than 1% except for the sample G2-15%-A where the relative error is around 3%; this sample has a compactness ratio equal to 96.1%.

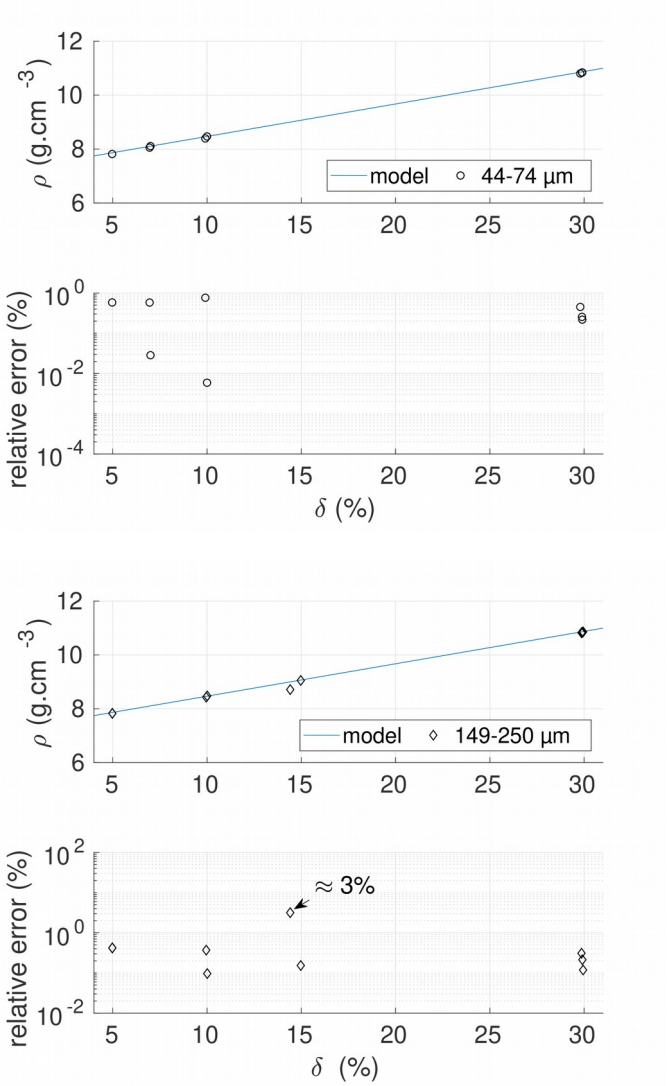

Fig1: Comparison between theoretical and experimental density as a function of the volume fraction of tungsten a) 44–74 µm b) 149–250 µm. For clarity uncertainty bars was not added, the uncertainty corresponds to the size of the data points.

The actual value of the volume fraction of tungsten is given by the following relation:

$$\delta_{exp} = \frac{\rho_{exp} - \rho_{SN} \cdot C}{\rho_W - \rho_{SN}} \quad (2)$$

whereby $C = \rho_{exp}/\rho$ is the compactness, ρ_{exp} is the experimental density and ρ is the theoretical density given by eq. (1). The value of compactness and actual volume fractions are reported in table 3. The uncertainty at 95% confidence in the density, compactness and volume fraction is equal to 0.2%. The compactness and actual volume fraction are reported in table 3.

The compactness C is one criterion which makes it possible to determine whether or not a sample has been correctly compressed. All samples have a compactness ratio greater than 99% (except the sample G2-15%-A with C = 96.1%) and thus the actual tungsten volume fraction corresponds to 0.4% of the specified value. For the sample G2-15%-A, the discrepancy between the volume fraction is 4%, but remains

acceptable. Therefore, we will use the theoretical volume fraction to refer to the samples.

8 samples G1 : 44-74 µm	C (%)	ρ (g/cm³)	δ (%)	<v> (m/s)	Z (Mrayl)
G1-5%-B	99.39	7.817	4.97	3211	25.10
G1-7%-A	99.38	8.055	6.96	3166	25.50
G1-7%-B	100.0	8.110	7.00	3166	25.68
G1-10%-A	100.0	8.468	10.00	3136	26.56
G1-10%-B	99.13	8.393	9.91	3136	26.32
G1-30%-A	99.35	10.802	29.80	3099	33.48
G1-30%-B	99.64	10.834	29.89	3099	33.57
G1-30%-C	99.70	10.840	29.91	3099	33.59
9 samples G2 : 149-250 µm	C (%)	ρ (g/cm³)	δ (%)	<v> (m/s)	Z (Mrayl)
G2-5%-A	99.58	7.831	4.979	3212	25.15
G2-5%-B	99.57	7.831	4.978	3212	25.15
G2-10%-A	100.0	8.478	10.01	3166	26.84
G2-10%-B	99.60	8.432	9.960	3166	26.70
G2-15%-A	96.10	8.714	14.42	3177	27.68
G2-15%-B	99.84	9.053	14.98	3177	28.76
G2-30%-A	99.56	10.825	29.87	2951	31.94
G2-30%-B	99.71	10.841	29.91	2951	31.99
G2-30%-C	99.84	10.856	29.95	2951	32.04

Table 3:Characteristics of samples; G1 corresponds to a grain size of 44–74 µm and G2 of 149–250 µm. Each sample name indicates the specified volume fraction. The uncertainty at 95% of confidence is equal to 0.09% for C and ρ, 0.1% for δ and 1% for velocity and impedance.

A. *Ultrasonic characterization*

Attenuation and velocity were measured as a function of the transmission frequency using the spectroscopic insertion and substitution method. A first reference signal is acquired in water, the test specimen is inserted and the transmitted signal is acquired. The spectrum of the acoustic transfer function is calculated (from the spectra of the two signals) whereby its phase allows deduction of the speed of sound and its amplitude the attenuation. This method is well described in literature, refer to [43-45] for example. The velocity is therefore deduced from the phase Φ (f), but is known to within ±k2π (k being an integer). The intercept of Φ (f) at f = 0 allows correction of this phase ambiguity [46]. This method appeared more robust than the method consisting of circularly time shifting the signals [44]. The effects of diffraction were corrected using the method describes in [47]

Due to the small diameter of samples (16 mm) and in order for the acoustic field to go entirely through the test specimens, we used probes with an active element diameter of 6 mm and with a beam diameter, at -6 dB, equal to 1.54 mm. The test specimens were then placed in the focal zone (the focal zone extending from N-1/3 N to N+2/3 N with $N=a^2/\lambda$, a being the radius and λ the wave length), at the beginning of the far field. Finally, the experiment was aligned by maximizing the reflected echoes.

We used two 5 MHz central frequency probes provided by Sonaxis Cie (Besançon - France). The emitter was excited with a five cycles tone-burst signal at several central frequencies: 3.5 MHz, 5 MHz and 6 MHz. This procedure enabled characterization of the test specimens from 3 MHz to 7 MHz without using other couples of probes thus avoiding issues due to misalignment. Furthermore, the electric excitation by tone-burst appeared to be more efficient than pulse excitation and rendered measurement with very high attenuating samples possible. This is not possible with pulse excitation. The measurement uncertainties are about 0.5% on velocity and attenuation at 95% confidence.

1. *Ultrasonic results for pure tin samples.*

We first measured the attenuation and velocity of the dense tin matrix material. The average attenuation for the seven tin samples is shown in Fig. 2

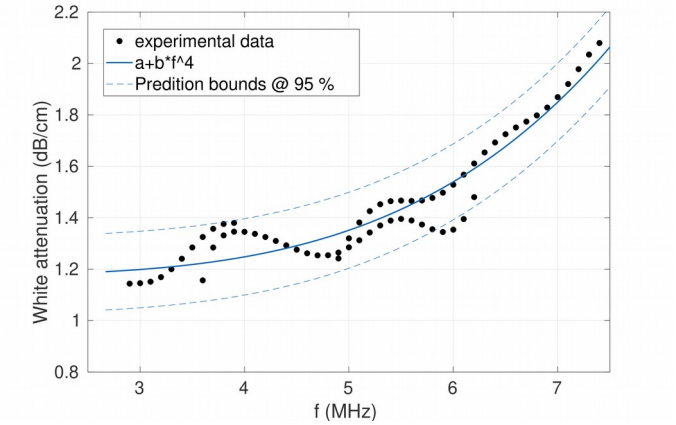

Fig 2: Average attenuation of pure white tin pellets as a function of the frequency.

We fitted the attenuation curve with the following model: $\alpha(f)=a+b\cdot f^4$ with α in dB/cm and f in MHz, and a = 1.176 (1.147; 1.205) and b = 2.805.10^{-4} (2.578.10^{-4}; 3.031.10^{-4}); the 95% confidence limits are in brackets. The adjusted R-square of the fit is 0.9053. The attenuation therefore depends on the fourth power of frequency that agrees with the Rayleigh theory [48]. The attenuation of tin is small and negligible in comparison with most other backing materials and the attenuation is mainly due to the multiple-scattering effects.

The dependence of the speed of sound with the frequency was found to be negligible. The mean speed of sound in a pure tin pellet is equal to 3270 m/s ± 4 m/s. The theoretical value is equal to 3300 m/s, i.e. a relative difference less than 1%.

2. *Samples with granulometry between 44-74 µm*

Figure 3 shows the attenuation of the 2 samples at 7% and the 3 samples at 30% for grain size G1. For sake of clarity, the results are only presented for the two extreme limits of the volume fraction. One observes a good manufacturing reproducibility. As the more the volume fraction increases, the more it becomes difficult to manufacture samples, the dispersion is greater for the volume fraction of 30%. Indeed, the greater the volume fraction, the more grains there will be, especially for the small grain size. For this reason, the apparent viscosity of the powder mixture increases and the mixing processes become harder to perform. Moreover, there are more surfaces of contact between grains of tungsten and

tin which renders mechanical cohesion more difficult. Reproducibility remains good even faced with these phenomena. We will therefore now present the mean attenuation and mean velocity of each volume fraction (Fig 4 and 5).

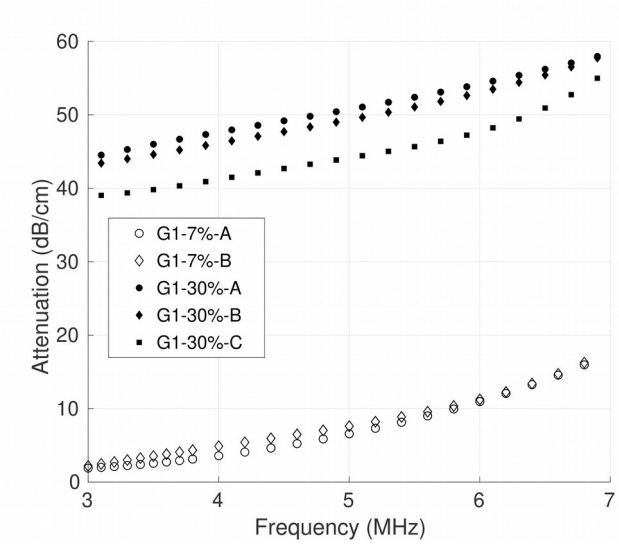

Fig 3: attenuation of 7% (2 samples) and 30% (3 samples) samples for the grain G1. The uncertainty in this case is the uncertainty of the spectroscopic method equal to 1 %.

Figures 4 and 5 shown respectively the mean attenuation and mean velocity for the samples with granularity G1 over 3 MHz to 7 MHz. Each curve results from the average data value (attenuation and velocity respectively) for each volume fraction; with the exception of the 5%, for which there is only one sample. Hence, the uncertainties take into account the uncertainty of ultrasonic measurements and the manufacturing reproducibility (equal to 1% both on velocity and attenuation), except for the 5% sample where only measurement uncertainty is taken into account.

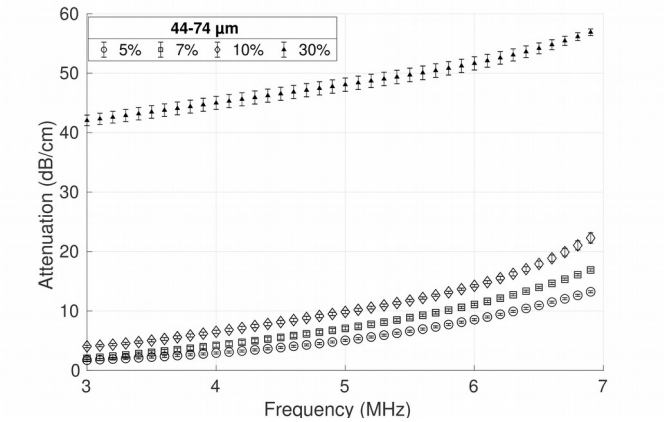

Fig 4: Mean attenuation as a function of the frequency of tin-tungsten samples for granularity G1.

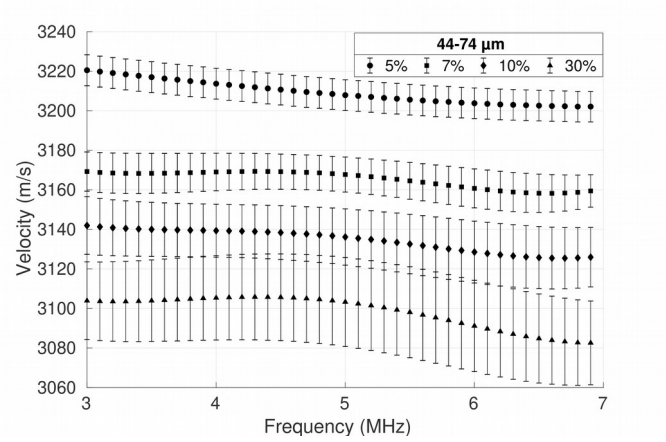

Fig 5: Mean velocity as a function of frequency of tin-tungsten samples for granularity G1.

The use of a small granulometry enables fine control of the ultrasonic properties. As expected, the attenuation increases slowly as the volume fraction increases from 5 to 10%. However, for the 30% backings, there is an important increase in attenuation. This is probably due to non-perfect contacts at tin-tungsten interfaces. Only this volume fraction allows exceeding attenuation values of 10 dB/cm. It is therefore necessary to use a larger grain size.

As expected, as the volume fraction increases, one observes a monotonic decrease in velocity. The variation of velocity with frequency is of the same order of magnitude as the uncertainty and may therefore be considered negligible (around 1% or about 30 $m.s^{-1}$). One therefore assumes that the velocity is constant over the frequency range and the average velocity (for each volume fraction) was used for modeling. The fact that the velocity is independent of the frequency allows us to use static models such as the Reuss model to compute the theoretical velocity and together with the density (eq. 1) obtain the theoretical impedance (refer to the next section).

3. *Samples with granulometry between 149 and 250µm*

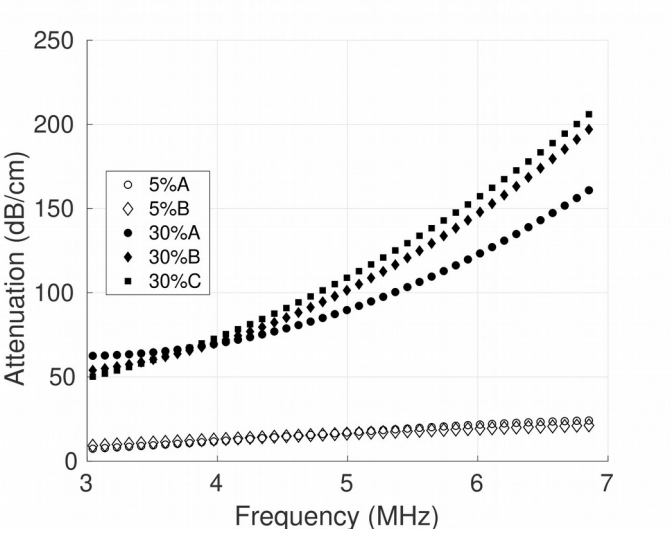

Fig 6: Attenuation of 5% (2 samples) and 30% (3 samples) samples for grain size G2. The uncertainty is around 1%.

Figure 6 shows the attenuation of the 2 samples at 5% and the 3 samples at 30% for grain size G2. As for grain size G1, for sake of clarity, the results are only presented for the two extreme limits of the volume fraction. One observes again a good manufacturing reproducibility. Nevertheless, as for grain size G1, the data for δ = 30% is more dispersed. The uncertainty is therefore mainly due to the manufacturing reproducibility.

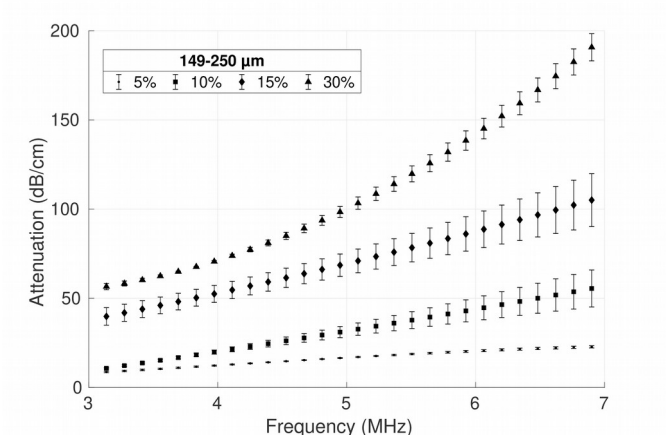

Fig 7: Mean attenuation as a function of frequency of tin-tungsten for granularity G2.

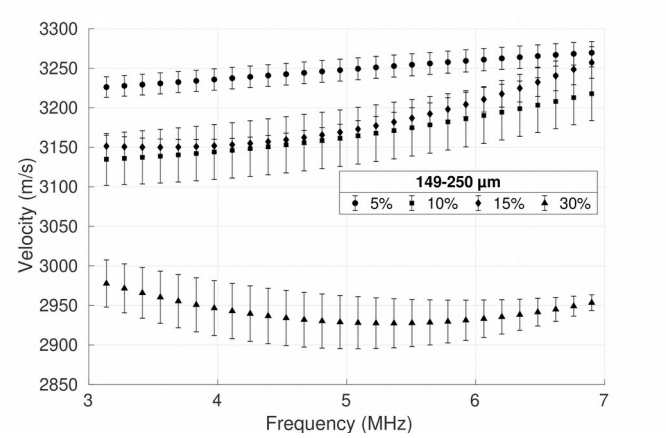

Fig 8: Mean velocity as a function of frequency of tin-tungsten samples for granularity G2.

Figures 7 and 8 show respectively the mean attenuation and the mean velocity for the samples with granularity G2 over 3 MHz to 7 MHz. As was the case for the smaller grain size G1, the average attenuation and velocity is used for each volume fraction. Again, the uncertainties take into account the uncertainty on both the ultrasonic measurements and the manufacturing reproducibility. One observes a monotonic increase in attenuation from 5% to 30% per volume of tungsten. The attenuation is always greater than 10 dB/cm so all samples meet the first condition.

It can be seen that the variation in velocity is negligible over the frequency range and the average value can therefore again be used. Although the mean velocity value of the 15% samples is too high compared to the expected value, all velocity values are, taking into account the uncertainties, in agreement with the model (Fig. 9). Only the mean velocity of the 30% samples is too low, but with a relative error of 5% this is still acceptable.

V. DISCUSSION

When the composite materials have a simple geometric condition such as iso-strain or iso-stress, the elastic moduli can be estimated based on rule-of-mixtures. Two typical rule-of-mixture models of elastic moduli are Voigt and Reuss models [49]. The iso-strain approach is known as the Voigt modulus that gives the upper limit of elastic moduli and the iso-stress approach is known as the Reuss modulus and gives the lower limit of elastic moduli. Elastic moduli of composite materials with (0–3) connectivity patterns for such backing materials are well modeled by the Reuss model [32]. The Reuss model enables prediction as follows:

$$M_B = \frac{M_W \cdot M_{Sn}}{\left((1-\delta)\cdot M_W + \delta \cdot M_{Sn}\right)} \qquad (3)$$

M, M_W and M_{Sn} are respectively the longitudinal modulus of the backing, tungsten and tin and are defined as follows: $M_x = \lambda_x + 2\mu_x$ with x standing for B, W or Sn;

λ_x and μ_x are the corresponding Lamé coefficients. They are equal to:

$$\lambda_x = \rho_x \cdot c_{x,p}^2 \quad \text{and} \quad \mu_x = \rho_x \cdot c_{x,s}^2$$

whereby $c_{x,p}$ is the compression wave velocity and $c_{x,s}$ is the shear wave speed. For tin c_p = 3270 m/s and c_s = 1700 m/s whereas c_p =5200 m/s and c_s = 2900 m/s for the tungsten [40, 41] . Knowing the density of the backing using equations 1 and 3 one obtains the longitudinal speed and impedance:

$$c_p = \sqrt{\left(\frac{M_B}{\rho}\right)} \quad (4)$$

and $$Z_B = \rho \cdot c_p = \sqrt{\left(M_B \cdot \rho\right)} \quad (5)$$

One can now compare the experimental values of speed and impedance with the theoretical values.

Figure 9 shows the comparison between the mean experimental velocities and the velocity calculated using the Reuss model. It can be seen that there is a very good agreement for both grain sizes G1 and G2. However, although the mean velocity of the three samples G2-30 % (A, B and C) is 100 m/s too low, it still remains an acceptable error at around 5% and, as already said, all the more so, as it is harder to manufacture higher volume fraction samples.

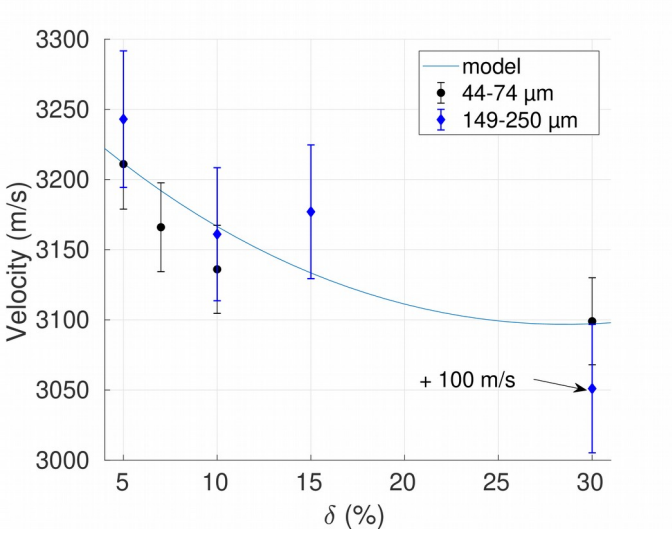

Fig 9: Comparison between experimental and theoretical velocities modeling using the Reuss's model (eq. 4.)

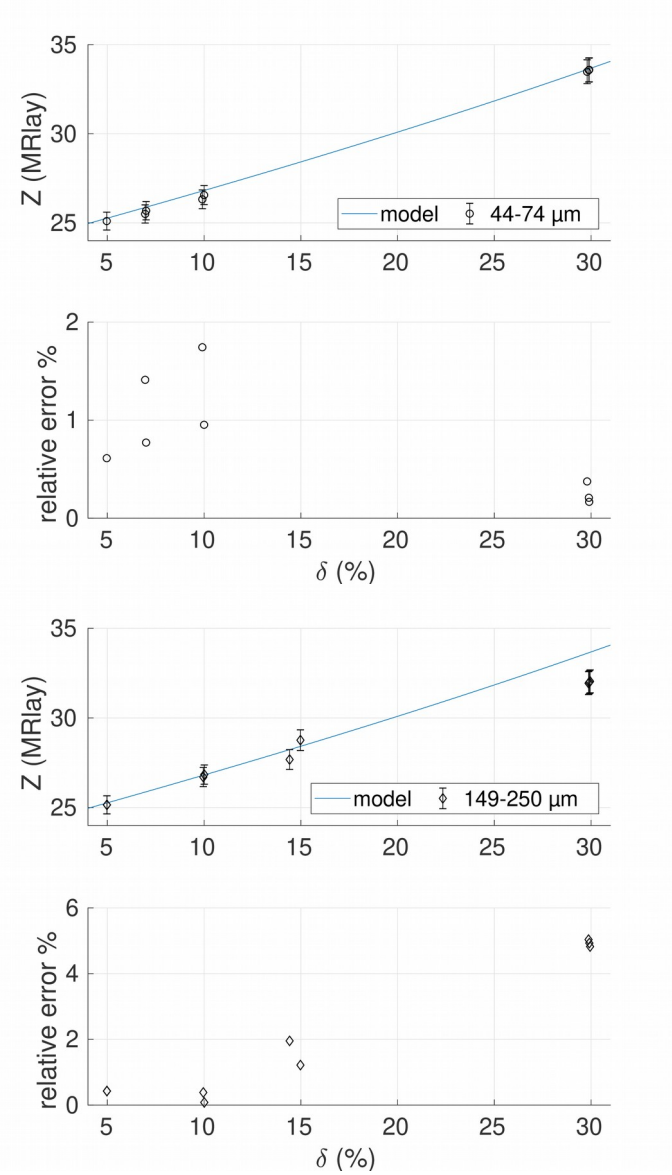

Fig 10: Comparison between experimental and theoretical impedance values (eq. 5)

As the velocity is in accordance with the model and the density is well predicted, then the impedance can also be well predicted as shown in figure 10. We are therefore able to manufacture new backing materials with the required properties. The mean attenuation and impedance of G2 samples are reported in table 4 at 3 MHz, 5 MHz and 7 MHz, and for four volume fractions.

	δ = 5%		δ = 10%		δ = 15%		δ = 30%	
	dB/cm	MRayl	dB/cm	MRayl	dB/cm	MRayl	dB/cm	MRayl
f = 3 MHz	10		11		40		57	
f = 5 MHz	17	25.15 (25.26)	31	26.77 (26.82)	68	28.22 (28.42)	98	31.99 (33.64)
f = 7 MHz	23		55		105		191	

Table4: Mean attenuation and mean impedance of samples made of G2 at 3 MHz, 5 MHz and 7 MHz for δ = 5, 10, 15 and 30%. The theoretical impedance is in brackets.

VI. *Aluminum tungsten backing.*

The main limitation of tin-tungsten materials is their operating temperature which is limited by the fusion temperature of tin (232 °C). They also have high impedance values which are indeed suitable for high-damped probes, but to increase the sensitivity of probes, especially at high temperatures, it is important to have materials with a lower impedance. To achieve this, one can use other metals with lower impedance values such as aluminum (17.33 MRayl) as matrix material for example. Moreover, contrasts between inclusion and matrix material can be expected with an increase in attenuation due to the increase in impedance. Figure 11 shows the expected impedance values of such composites; one can expect to cover an interesting range from 17 to 25 MRayl, but this impedance range can be reduced by increasing porosity. To do this, one could simply reduce the compression force.

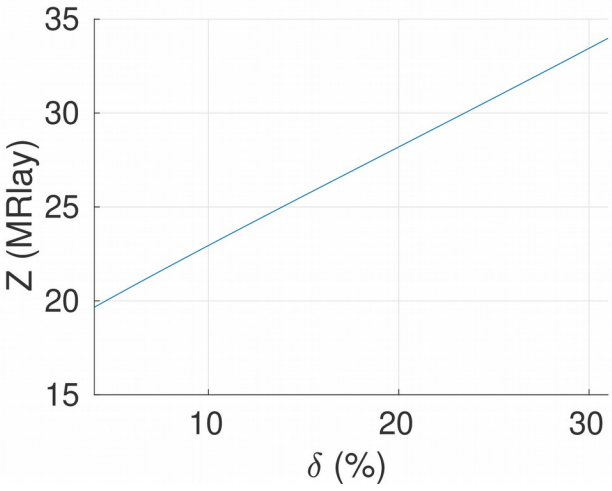

Fig 11: Expected values of impedance for Al/W composite as a function of the volume fraction.

We thus produced an aluminum sample with 5% per volume of tungsten, but only compressed at 40 kN (i.e. p = 2 kbar for a sample of 16 mm in diameter). The compression characteristics are the following:

- grain size G1: 44–74 um,

- compression load = 40 kN,
- compression speed = 0.1 mm/min,
- thickness = 4.3 mm,
- diameter =16.1 mm,
- volume fraction δ = 5%.

As was the case for the tin-tungsten samples, we measured the density (ρ = 3.244 g/cm^3 corresponding to a compactness ratio of C = 91.89%) and deduced the actual volume fraction which is equal to δ = 4.59%. With compactness equal to 91.9%, it is normal not to have an actual volume fraction equal to that expected. Indeed, the volume of air is not negligible and this is why the thickness is higher than expected (4.3 mm for 4 mm expected).

We then measured the attenuation and velocity and calculated the impedance; both are shown in figure 12. Since porosity reduces density and increases attenuation, a sample with a very high attenuation (greater than 138 dB/cm) and a lower impedance ranging from 8 MRayl and 10 MRayl between 3.5 MHz and 6 MHz was obtained. Moreover, it may be noted that the impedance is not constant due to dispersion of the velocity, which is not negligible as the multiple scattering effects are higher. In this case, due to the very high attenuation, the maximum characterization frequency is 6 MHz.

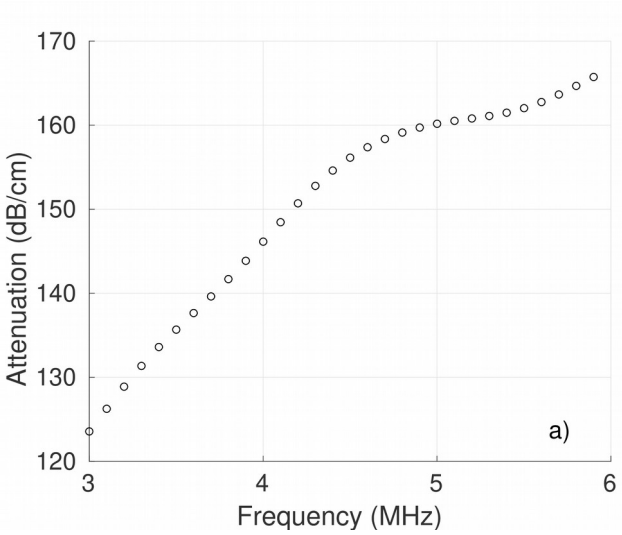

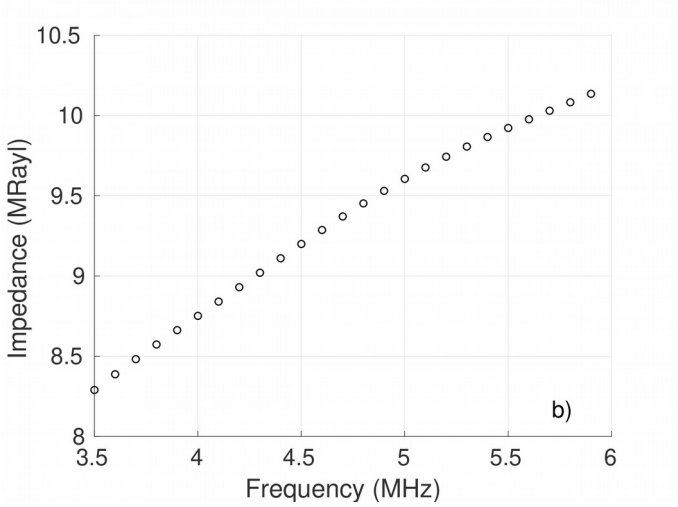

Fig 12: a) Attenuation and b) acoustic impedance of the Al-W composite versus frequency.

By compressing at a lower pressure, one obtained a sample with a lower impedance, but perhaps also with a lower mechanical strength. To test its temperature resistance, the sample was annealed for 12 hours at 550 °C. No defects were detected and furthermore, we did not notice any decrease in porosity and therefore no sintering (Figure 13).

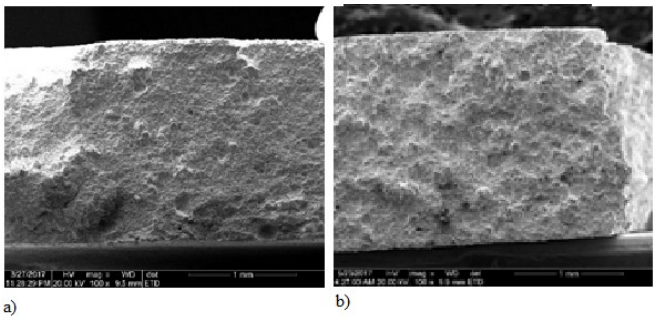

Fig 13: SEM image of the Al/W(5%) sample a) before annealing and b) after 12 hours of annealing at 500°C

VII. CONCLUSION AND PERSPECTIVE

Metal composite materials are limited only by their fusion temperature. With careful selection, they can therefore be used as backing elements in high-temperature applications. Furthermore, they have similar thermal expansion coefficients to those of electrodes which makes this material suitable for ultrasonic probe manufacturing by reducing the stress at the backing/piezoelectric interface. The metal composites are made by mixing two metal powders, the first being the matrix material and the second the inclusions. Seventeen tin-tungsten composites were manufactured; eight with a tungsten powder with a grain size of 44–74 µm and nine with a grain size of 149–250 µm. The density of each sample was measured and compared with the theoretical density, with compactness higher than 99% (except for only one sample with C = 96.51%), an excellent agreement was noted with the theoretical density values.

Attenuation and velocity were measured, between 3 MHz and 7 MHz, in transmission using the ultrasonic spectroscopy method. The impedance of each sample was then deduced. The agreement between experimental values and those obtained with the Reuss's model is excellent.

When larger grains are used (because for a specified volume fraction, there will be fewer grains), homogeneity problems could occur, but no such problems were encountered. Moreover, only the largest grain size G2 provides a backing with adapted attenuation (>10 dB/cm), and this regardless of the volume fraction. The attenuation is therefore all the more important as the grain size increases in exactly the same way as for polymer-based backings [32].

Recent works showed that porous ceramics can be used as acoustic backing for high-temperature applications [22, 24, 25]. The volume fraction and the pore size enable control of the attenuation and impedance of these backing materials. The impedance of these materials ranges from 20 MRayl to 34 MRayl for a porosity between 30% and 10%. Between 1.5 MHz and 4.5 MHz, the attenuation is between 20 dB/cm and 60 dB/cm. At 3 MHz, the attenuation ranges from 5 dB/cm to 25 dB/cm and at 4.5 MHz, the attenuation is between 5 dB/cm and 40 dB/cm for a pore size between 96 µm and 160 µm. The acoustic properties of these materials are good and they are suitable for operation at temperatures as high as 800°C. However, they are difficult to manufacture.

The impedance of tin-tungsten backings is between 25 MRayl and 31 MRayl for a volume fraction of tungsten ranging from 5% to 30%. At 3 MHz, the attenuation is between 10 dB/cm and 57 dB/cm and at 4.5 MHz, the attenuation is between 15 dB/cm and 85 dB/cm. They therefore have an impedance comparable with that of porous backings, but with a higher attenuation. However, they are limited to operation at a moderate temperature of around 230 °C. The main goal of this paper was to examine the ability of using metal composites for high-temperature applications. We carried out the study with Sn-W composites because of the tin malleability allowing easy compression for such composites. However, there are a lot of other metallic powders that could be used as matrix material in order to control the impedance, attenuation and, of course, the operating temperature. We therefore produced a sample of Al-W with a volume of tungsten of 5%. By compressing it at a relatively low pressure (2 kbar), we obtained a sample with a porosity of about 9% allowing us to obtain an impedance between 8 and 10 MRayl and an average attenuation of about 156 dB/cm at 4.5 MHz. It should be noted that aluminum has malleability and ductility that allows it to be compressed relatively easily.

Finally, in this work, we did not take many precautions when compressing the samples although there are simple actions which may be applied to improve the manufacturing process such as incorporating plasticizers or operation under a slight vacuum. These improvements should be adopted in future experiment.

Acknowledgements :
We would like to thank Mr. Guillaume Pierre from the company Sonnaxis (Besançon, France) for providing us with the ultrasonic transducers and for the verification of the KLM models. We also thank the reviewers who helped to improve the paper.

REFERENCES

[1] M. Budimir, M. Mohimi, C. Selcuk, et al, "High temperature nde ultrasound transducers for condition monitoring of superheated steam pipes in nuclear power plants". In : Proceedings of the International Conference Nuclear Energy for New Europe, Bovec, Slovenia, 2011, pp. 501-1.

[2] J. W. Griffin, G. J. Posakony, R.V. Harris, et al, "High temperature ultrasonic transducers for in-service inspection of liquid metal fast reactors". In : 2011 IEEE International Ultrasonics Symposium. IEEE, Orlando, USA, 2011. pp. 1924-1927.

[3] F. BENOIT, Ultrasonic Nondestructive Testing in Oil wells 2002.

[4] KOBAYASHI2012 Ultrasonic Transducers Materails and Design Transducers for non-destructive evaluation at high temperatures, in K. NAKAMURA, (ed.). *Ultrasonic transducers: Materials and design for sensors, actuators and medical applications*. Elsevier, 2012.

[5] R. Kazys, A. Voleisis, et B. Voleisiene, "High temperature ultrasonic transducers". Ultragarsas, vol. 63, no 2, pp. 7-17, 2008.

[6] T. Uchimoto, T. Takagi, G. Domann, et al. "Development and Performance Evaluation of High Temperature Electromagnetic Acoustic Transducer". 2016. available at : https://lib.dr.iastate.edu/qnde/2016/abstracts/192/

[7] L. Lynnworth. "Ultrasonic measurements for process control: theory, techniques, applications". Academic press, 2013.

[8] T. Lambert, E. Muller, E. Federici, E. Rosenkrantz, J-YFerrandis, X.Tiratay, V. Silva, D. Machard, G. Trillon,"REMORA 3: The first instrumented fuel experiment with on-line gas composition measurement by acoustic sensor" 2011 2nd International Conference on Advancements in Nuclear Instrumentation, Measurement Methods and their Applications, Ghent, Belgium, 2011. pp.1-6, 2011, IEEE.

[9] E. Rosenkrantz, JY. Ferrandis, F. Augereau, T. Lambert, D. Fourmentel, X. Tiratay, "An innovative acoustic sensor for in-pile fission gas composition measurements," IEEE Transactions on Nuclear Science, vol. 60,no. 2, pp. 1346- 1353, 2013

[10] C. Bosyj, N. Bhadwal, T. Coyle, et al. "Brazing Strategies for High Temperature Ultrasonic Transducers Based on LiNbO3 Piezoelectric Elements". Instruments, 2019, vol. 3, no 1, december, p.2, 2018.

[11] S. Zhan and al, "piezoelectric accelerometers for ultrahigh temperature application" Applied physics letters Vol. 96 pp. 013501-013506, 2010, Doi:10.1063/1.3290251

[12] M. N. Hamidon "High-Temperature 434 MHz Surface Acoustic Wave Devices Based on GaPO4" IEEE transactions on ultrasonics, ferroelectrics, and frequency control, vol. 53, no. 12, december 2006. **DOI:** 10.1109/TUFFC.2006.194

[13] N.D. Patel and al"High Frequency-High temperature ultrasonic transducers" review of progress in Quantitative Nondestructive Evaluation. Vol.9 pp.823-828, 1990, https://doi.org/10.1016/0308-9126(90)92152-Q

[14] Mrase, "High Temperature Ultrasonic Transducers NDT," Vol. 1 No. 09 September, 1996.

[15] A. Mcnab, K. J. Kirk, et A. Cochran. "Ultrasonic transducers for high temperature applications". IEE Proceedings-Science, Measurement and Technology, vol. 145, no 5, p. 229-236, 1998.

[16] A. Dhutti, S. A. TUMIN, T. H. GAN, et al, "Comparative study on the performance of high temperature piezoelectric materials for structural health monitoring using ultrasonic guided waves". In : Proceedings of the 7th Asia-Pacific Workshop on Structural Health Monitoring, Hong Kong, China, 2018, pp. 12-15.

[17] A. Baba, SEARFASS, T. Clifford, et B. R., "Tittmann.High temperature ultrasonic transducer up to 1000 C using lithium niobate single crystal". Applied Physics Letters, vol. 97, no. 23, p. 232901, 2010.

[18] C. T. Searfass, C. PHEIL, K. Sinding, et al. "Bismuth titanate fabricated by spray-on deposition and microwave sintering for high-temperature ultrasonic transducers". IEEE transactions on Ultrasonics, Ferroelectrics, and Frequency control, vol. 63, no 1, pp. 139-146, 2015.

[19] Y. TRIVEDI, B.R. TITTMANN, B. R., C. BATISTA, Field deployable spray-on ultrasonic coatings for high-temperature applications. In : *AIP Conference Proceedings*. AIP Publishing, 2019. p. 060008.

[20] O. Gatsa, P. Combette, E. Rosenkrantz,et al. "High-Temperature Ultrasonic Sensor for Fission Gas Characterization in MTR Harsh Environment". IEEE Transactions on Nuclear Science, vol. 65, no. 9, pp. 2448-2455, 2018.

[21] D. A. Parks, S. Zhang, et B. R. Tittmann. "High-temperature (> 500/spl deg C) ultrasonic transducers: an experimental comparison among three candidate piezoelectric materials". IEEE transactions on Ultrasonics, Ferroelectrics, and Frequency control, vol. 60, no. 5, pp.1010-1015, 2013.

[22] Mohammad Hossein Amini and al "Porous Ceramics as BackingElement for High-Temperature Transducers" IEEE Transactions on Ultrasonics, Ferroelectrics, and Frequency Control, vol. 62, no. 2, February 2015, DOI: 10.1109/TUFFC.2014.006711

[23] A. H. Amini, A. N. Sinclair, et W. T. Coyle. "High temperature ultrasonic transducer for real-time Inspection".Physics Procedia, vol. 70, pp. 343-347, 2015.

[24] M. H. Amini and al "A new high temperature ultrasonic transducer for continuous inspection" IEEE Transactions on Ultrasonics, Ferroelectrics, and Frequency Control, 2016, **DOI:** 10.1109/TUFFC.2016.2519348

[25] M. H. AMINI, *Design and Manufacture of an Ultrasonic Transducer for Long-term High Temperature Operation*. 2015. Thèse de doctorat.

[26] J. Souquet, P. Defranould, et J. Desbois. "Design of low-loss wide-band ultrasonic transducers for noninvasive medical application". IEEE transactions on sonics and ultrasonics, vol. 26, no 2, pp 75-80. 1979.

[27] C. Desilets, J. D. Fraser, et G. K. Kino. "The design of efficient broad-band piezoelectric transducers," IEEE Transactions on sonics and ultrasonics, vol. 25, no 3, pp. 115-125, 1978.

[28] G. Kossoff. "The effects of backing and matching on the performance of piezoelectric ceramic transducers".IEEE Transactions on sonics and ultrasonics, vol. 13, no. 1, pp. 20-30, 1966.

[29] M; G. SILK, Ultrasonic transducers for nondestructive testing. 1984.

[30] H. Kwun, W.D. Jolly, G. M. Light, et al. "Effects of variations in design parameters of ultrasonic transducers on performance characteristics". Ultrasonics, vol. 26, no. 2, pp. 65-72, 1988.

[31] C. M. Sayers "Ultrasonic properties of transducer backings." Ultrasonics, Vol.22, No.2, pp. 57-60, 1984. https://doi.org/10.1016/0041-624X(84)90022-2

[32] M. G. Grewe, T. R. Gururaja, T. R. Shrout, et al. "Acoustic properties of particle/polymer composites for ultrasonic transducer backing applications". IEEE transactions on ultrasonics, ferroelectrics, and frequency control, vol. 37, no. 6, pp. 506-514, 1990.

[33] S. Lees and al "Acoustic Properties of Tungsten-Vinyl Composites." IEEE, Vol. 20, No. 1, 1973, DOI: 10.1109/T-SU.1973.29713

[34] J. D. Larson, et J. G. Leach. "Tungsten-Polyvinyl Chloride Composite Materials-Fabrication & Performance," In : 1979 Ultrasonics Symposium. IEEE,USA, New Orleans, pp. 342-345, 1979.

[35] Y. B. Cohen, D. A. Stubbs, et W. C. Hoppe. "Multiphase backing materials for piezoelectric broadband transducers". The Journal of the Acoustical Society of America, vol. 75, no. 5, pp. 1629-1633, 1984.

[36] S. Rokhlin and al "Acoustic properties of tungsten-tin composites." JASA, Vol. 69, No. 1505, 1981. https://doi.org/10.1121/1.385788

[37] Royer99 ROYER, Daniel et DIEULESAINT, Eugene. *Elastic waves in solids II: generation, acousto-optic interaction, applications*. Springer Science & Business Media, 1999.

[38] Ferroperm Data properties of ceramic are availble at https://www.meggittferroperm.com/materials/

[39] Onda : http://www.ondacorp.com/tecref_acoustictable.shtml

[40] A. R. Selfridge. "Approximate material properties in isotropic materials.IEEE transactions on sonics and ultrasonics, vol. 32, no. 3, pp.381-394, 1985.

[41] S. Kino, "Acoustic Waves: Devices, Imaging, and Analog Signal Processing", Prentice-Hall, ISSN 1050-2769, ISBN 0130030473, 9780130030474, 1987.

[42] F. V. LENEL, *Powder metallurgy: principles and applications*. Metal Powder Industry, 1980.

[43] W. Sachse, Y. Pao. "On the determination of phase and group velocities of dispersive waves in solids". Journal of applied Physics, vol. 49, no. 8, pp. 4320-4327, 1978.

[44] P. HE, J. Zheng. "Acoustic dispersion and attenuation measurement using both transmitted and reflected pulses". Ultrasonics,vol. 39, no. 1, pp. 27-32, 2001.

[45] H. Wang, W. Cao."Improved ultrasonic spectroscopy methods for characterization of dispersive materials". IEEE transactions on ultrasonics, ferroelectrics, and frequency control, vol. 48, no. 4, pp.1060-1065, 2001.

[46] P. Droin, G. Berger, P. Laugier. "Velocity dispersion of acoustic waves in cancellous bone". IEEE transactions on ultrasonics, ferroelectrics, and frequency control, vol. 45, no 3, pp. 581-592, 1998

[47] G. Leveque,and al,"Correction of diffraction effects in sound velocity and absorption measurements. Measurement Science and Technology, vol. 18, no. 11, pp. 3458, 2007.

[48] J. Saniie, and al. "Quantitative grain size evaluation using ultrasonic backscattered echoes". The Journal of the Acoustical Society of America, vol. 80, no 6, pp. 1816-1824, 1986.

[49] K. S. Kim, K. Lee, et al. "Dependence of particle volume fraction on sound velocity and attenuation of EPDM composites".Ultrasonics, vol. 46, no 2, pp. 177-183, 2007.